CHALMERS
UNIVERSITY OF TECHNOLOGY

Load effects in beams with corrugated webs: Numerical study

NORDIC STEEL 2024
The 15th Nordic Steel Construction Conference,
June 26–28, 2024, Luleå, Sweden

Load effects in beams with corrugated webs

Numerical study

Fatima Hlal*[,a,b], Mohammad Al-Emrani[a]

[a]Chalmers University of Technology, Department of Architecture and Civil Engineering, Sweden
[b]WSP, Bridge Department, Sweden
fatima.hlal@chalmers.se, mohammad.al-emrani@chalmers.se

ABSTRACT

Corrugated steel web girders have emerged as a promising choice in bridge construction due to their benefits in reducing material. Fatigue is a common cause of failure in structures subjected to cyclic loading such as bridges. Evaluating the fatigue strength of corrugated web girders presents challenges due to the complex geometry and load transfer mechanism. Unlike conventional plate-girders with flat webs, the shape of corrugated webs affects the stress distribution in girder flanges when it is subjected to bending and shear. Previous research has noted the uneven stress distribution along the flange width. However, these studies have not distinctly separated the various load effects that collectively contribute to this uneven stress distribution. Such separation is particularly important for understanding the fatigue behaviour of these girders and identifying the relevant stress components to be used in fatigue design. The goal of this study is to identify different load effects in the flanges of corrugated web girders under bending and shear. Four finite element models of beams with corrugated webs loaded in four-point bending are constructed, validated, and the load effects from bending and shear are separated and analysed. The study identifies, besides the membrane stress effect, three bending load effects in the flanges. The first bending effect is the transverse bending caused by shear flow. The second bending effect is local transverse bending caused by the uneven contribution of the web to the beam section modulus. The last bending effect is global transverse bending. These bending effects are influenced by various factors such as the number of the corrugations per shear span, where the support and load are positioned (whether on an inclined or flat fold), and the symmetry within the shear span. These variables collectively impact how stress is distributed in the flange, highlighting the complexity of the behaviour of corrugated web girders.

Keywords: Corrugated web, Fatigue, Transverse bending, Stress distribution

INTRODUCTION

Corrugated web beams have gained increasing interest in bridge applications due to their demonstrated economic efficiency (1). This is due to the fact that employing a corrugated web allows for thinner plates in the web with reducing the requirement on vertical stiffeners, lowering the cost of material and fabrication (2).

The structural behaviour of beams with corrugated webs under static loads has received relatively good attention. Previous experimental and numerical investigations demonstrated that the corrugated web profile has a significant influence on the distribution of axial stress in the web. Normal stress in the web decreases dramatically a short distance below the web-flange junction and is non-existent in the major section of the web (3), a phenomenon known as "the accordion effect." As a result, it is typical in the design of these girders to assume that only the flanges carry the bending moment, while the corrugated web carries the shear force (3), (4). In a related context, Inaam and Upadhyay (5) carried out a numerical study on corrugated I-girders with compact and laterally constrained flanges

with the goal of quantifying accordion effects. According to the study, the web can contribute to bending resistance with a minimum web participation factor of 10% (i.e. equivalent to a flat web with a thickness 0.1 tw) under certain conditions stated in their paper (5).
With reference to fatigue loading, compared to beams with flat webs, the corrugated web shape introduces stress concentration points, typically found at the corners of corrugations. These points have specific fatigue strength properties and are influenced by load effects that differ from those seen in flat web girders. Previous experimental tests have shown fatigue cracking, notably at the intersection of the inclined and flat folds (6), (7), (8), represented as the Point S in *Fig. 1*.

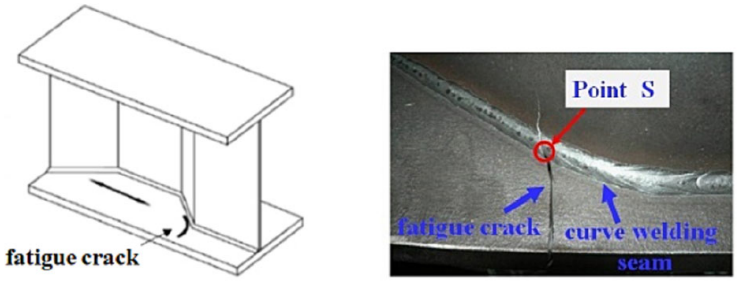

Fig. 1 Location of fatigue crack in corrugated web beams **(6)**

Stress distribution in the flanges of corrugated web girders has been examined in previous research, which showed that a corrugated web I-girder twists out-of-plane under the action of in-plane primary bending moment and shear (4). The shear stress within the corrugated web generates a transverse bending moment that results an extra bending stress induced in the flange (9), see *Fig. 2*. Linder and his coworkers were the first to show that corrugated web I-girders under moment and shear experience flange transverse displacements and flange transverse bending stresses (4). Abbas et al. (4) developed and validated a theoretical method called “The fictitious load method” as an analytical tool for evaluating flange transverse bending in corrugated web I-girders and other piecewise linear folds, e.g., triangular, and rectangular. This method assumes that the shear is carried entirely by the web and the bending is carried entirely by the flanges and indicates that the in-plane bending behaviour can be solved independently from the out-of-plane torsional behaviour (4). Kövesdi et al. (10) further investigated this phenomenon and derived an equation to quantify the transverse bending generated by shear flow. The authors observed that the distribution and magnitude of transverse bending depended on the type of loading as well as the on the location of supports and loading in relation to the corrugation (10). Another study, conducted by Anami et al. (11), demonstrated that in addition to the primary bending of the beam, the flanges are subjected to transverse bending (i.e., in the plane of the flange, refer to *Fig. 2*) occur even in a region of constant primary bending moment (12). This observation was also made by Abbas et al. (4), indicating that there is transverse bending of the flange due to the uneven contribution of the web to the beam section modulus.

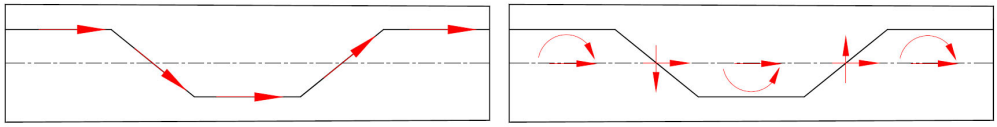

Fig. 2 An illustration of the transverse bending induced by shear flow in corrugated web beams.

The goal of this study is to identify and - if possible - separate these load effects; in-plane bending, out-of-plane bending due to shear flow, and out-of-plane bending due to uneven web contribution to the beam section modulus. A good understanding of the mechanisms behind these different load effects and how they might interact is essential for a more refined understanding of the fatigue performance of girders with corrugated webs. Numerical analysis is performed on four girders loaded in four-point bending, varying the support and load locations, as well as the number of corrugations in the shear span. The models are validated with hand calculation using Euler–Bernoulli beam theory neglecting the web in the calculation of the second moment of area. The various load effects are separated, and their individual contributions to the stress value at S-point under pure bending and combined shear-bending, are evaluated.

1 NUMERICAL STUDY

1.1 Numerical model description and validation

Four finite element models are constructed. The four models share the same corrugation wave arrangement as illustrated in *Fig. 3*. The corrugation configuration was adopted from Kövesdi et al. (8). The four models are subjected to the same shear force (50kN). Table 1 and *Fig. 3* depict the models' geometries and show the locations of supports and load application points. In Girder 1 and Girder 2, both the loads and supports are located on a flat fold. Girder 1 features a whole number of corrugations (4 waves) per shear span, whereas Girder 2 features 5.5 waves per shear span. Girders 3 and 4 have the point loads and supports located on an inclined fold, featuring 4 and 4.5 waves per shear span, respectively.

Table 1 Geometric configurations of studied models along with loading and supporting positions.

	Length [m]	Load on	Support on	No. of waves	Shear force [kN]
Girder 1	8.625	Flat fold	Flat fold	4	50
Girder 2	10.875	Flat fold	Flat fold	5.5	50
Girder 3	8.625	Inclined fold	Inclined fold	4	50
Girder 4	9.375	Inclined fold	Inclined fold	4.5	50

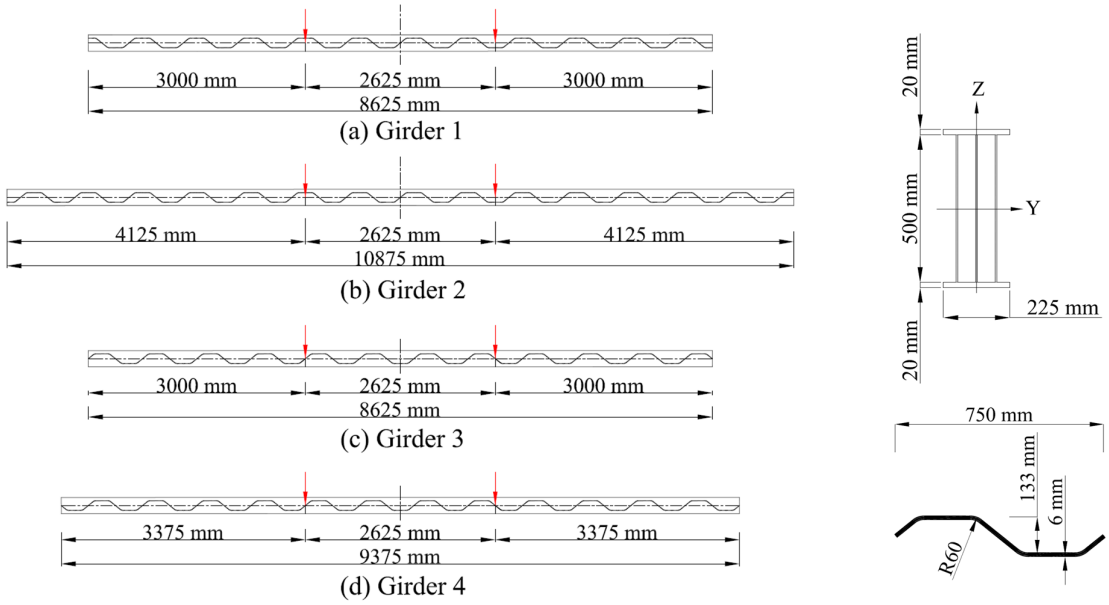

Fig. 3 Illustration of the studied girders with the corrugation configuration.

Abaqus CAE 2020 is used to construct and analyse the finite element models. *Fig. 4* shows the model for Girder 1, depicting a simply supported beam under four-point bending. It incorporates a pinned support at one end and a roller support at the other. To mesh the model, a quadratic tetrahedral solid element, C3D10, which is known for its precise automated meshing and good general-purpose properties is employed (13). To minimize local effects under concentrated loads at the supports, two stiffeners are added in the model at each end. Additionally, two more stiffeners are modelled beneath the point loads for the same reason. However, these are intentionally cut short at the bottom flange to avoid any influence of the stiffeners on the stress concentration in the bottom flange (even though these are not covered in this paper, these models are used as global models for sub models that are later used to evaluate the effective notch stress at the weld toe).

The boundary conditions set are intended to allow beam bending in both the primary plane (web plane) and the lateral plane (flange plane). *Fig. 4* illustrates the applied boundary conditions. The bottom flange's two edges are constrained vertically (Z-direction), while the midpoints of the four

edges of both top and bottom flanges are constrained laterally (Y-direction). Additionally, the midpoint of one side of the bottom flange edge is constrained longitudinally (X-direction).

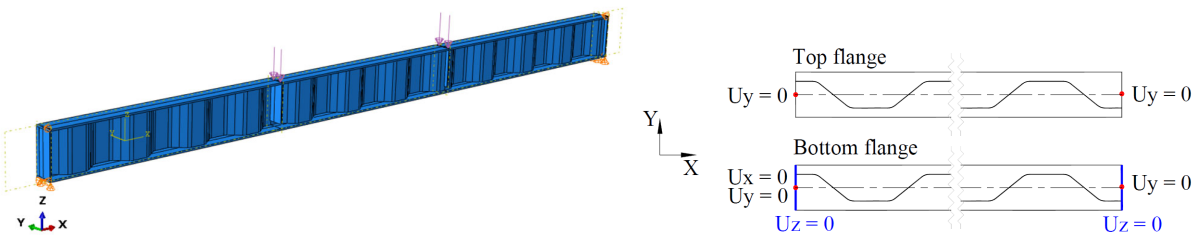

Fig. 4 FE model with the applied boundary conditions

To validate the models, the deflection and average stress on the bottom surface of the bottom flange in the pure bending zone are compared to hand calculations. The deflection is determined as: $\Delta = \frac{Pa}{8EI}\left[\frac{4}{3}a^2 + 2ab + \frac{b^2}{2}\right]$ where Δ: mid span vertical deflection (mm). P: total applied load on the girder (kN). a: shear span, i.e. distance from the support to the load application point (mm). E: Young's modulus (GPa). I: moment of inertia of the cross section neglecting the web contribution (mm^4). b: distance between the two-load application P (mm).

The validation of Girder 1 is shown in Table 2. As can be seen, both the deflection and the average stress (measured at the middle of the inclined and flat folds in the pure bending region, *Fig. 5*) accord well with hand calculation.

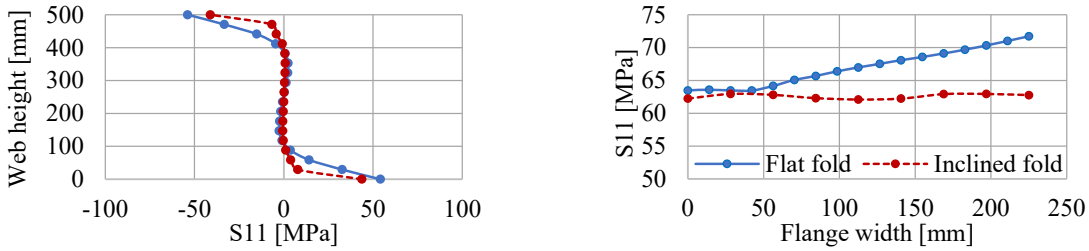

Fig. 5 Stress distribution along the web and the flange in Girder 1.

Table 2 Finite element model validation for girder 1

	FEM	Hand calculation	difference
Average normal stress at bottom surface of bottom flange [MPa] (Inclined fold)	62.09	66.5	6%
Average normal stress at bottom surface of bottom flange [MPa] (Flat fold)	66.96	66.5	1%
Midspan deflection [mm]	9.55	9.6	1%

1.2 Load effects in the flange

The normal stresses S11 along the two edges of the tension flange bottom surface are initially plotted. *Fig. 6* shows these results for Girder 1; the blue line denotes S11 along the south edge, while the red line represents S11 along the north edge. As can be demonstrated from *Fig. 6*, the stresses along the flange width are not uniform in any section along the beam. This non uniform distribution can be even seen in the constant moment region where the shear stress is zero. The stresses along the two flange edges are alternating which indicates transverse bending around the minor beam axis. This bending can be also seen when modelling a flange under tension, indicating that it is caused by the uneven web contribution to the beam section modulus. In the combined shear-bending region, additional transverse bending from shear flow is generated. The shape and the sign of these two-transverse bending effects are discussed further in the following sections.

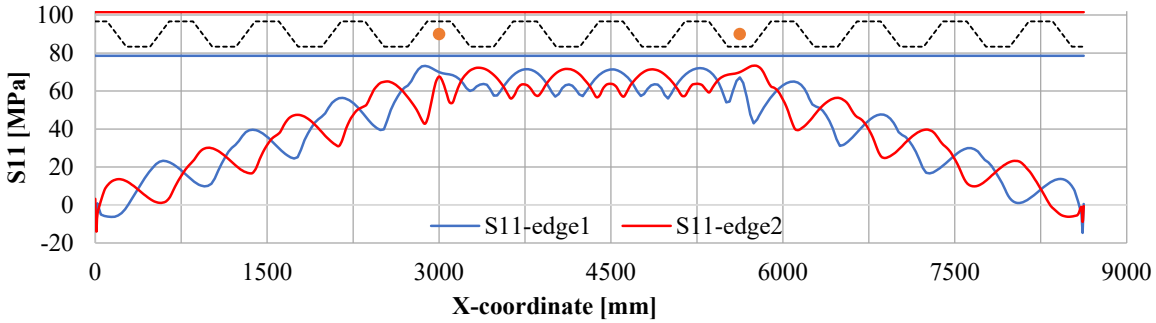

Fig. 6 S11 along the two edges of bottom flange in Girder1

To further process the results and identify different actions contributing to the stresses in the flanges, the stresses at any section along the flange were divided into three components: membrane stress, bending from the uneven web contribution to the beam section modulus, and bending from shear flow. *Fig. 7* shows an illustration of these three components. The membrane and bending stresses can be calculated as $\frac{S11.edge1+S11.edge2}{2}$ and $\frac{S11.edge1-S11.edge2}{2}$, respectively. The bending stress from the uneven web contribution to the beam section modulus can be estimated from the pure bending (constant moment) region. This bending moment should give tensile and compressive stresses along flange edges with equal and opposite values (i.e. fluctuating around zero). Similar bending stresses due to web uneven contribution exist along the shear spans but their values are scaled following the gradient of primary bending moment.

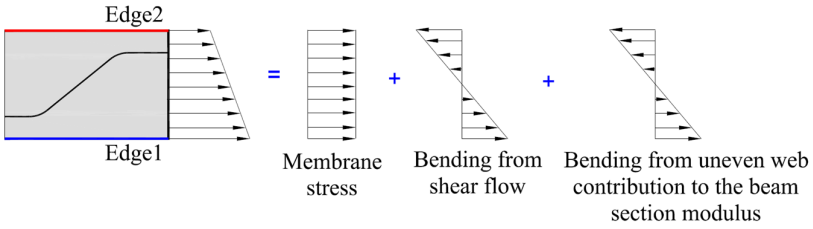

Fig. 7 An example of the stress components at any section along the flange

Fig. 8 depicts Girder 1 separated load effects. In this girder, the load and the supports are positioned on the flat fold, and the shear span has an integer number of corrugations. As can be seen in *Fig. 8*, the first bending effect which is coming from uneven web contribution to the beam section modulus always compresses the flange side closest to the flat fold. This effect is further illustrated in *Fig. 9* and will be discussed in section 3. The second bending effect which is caused by shear, exhibits two half-sine waves per corrugation with a stress value of roughly 10MPa. According to Kövesdi (10), this value can be calculated using *Fig. 10*a which gives a value of 11.5MPa. The obtained value from the FE analysis is believed to be lower owing to the radius of corrugation which is included in the FE-model, resulting in a reduction in T1 in *Fig. 10*.

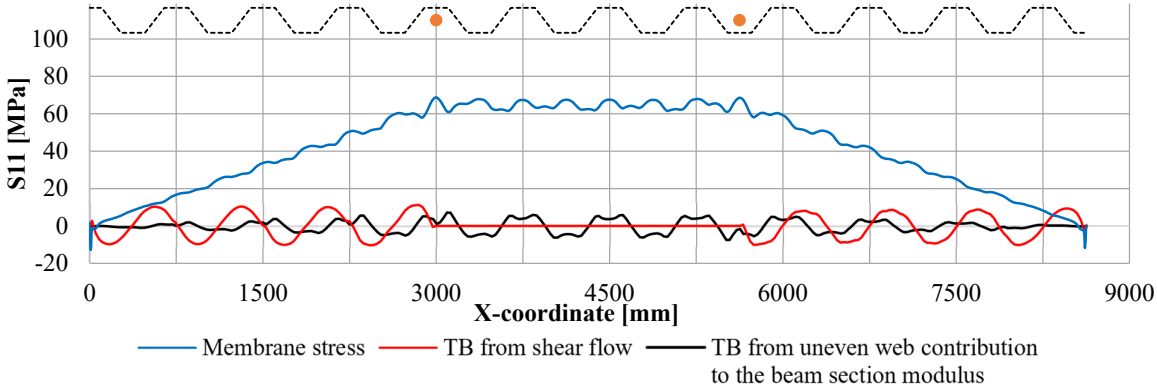

Fig. 8 Separated load effects for Girder 1

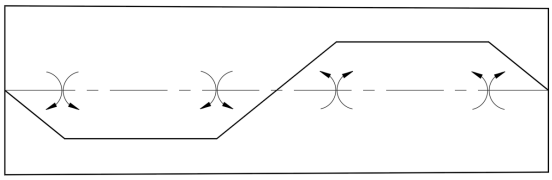

Fig. 9 Illustration of transverse bending from uneven web contribution to the beam section modulus.

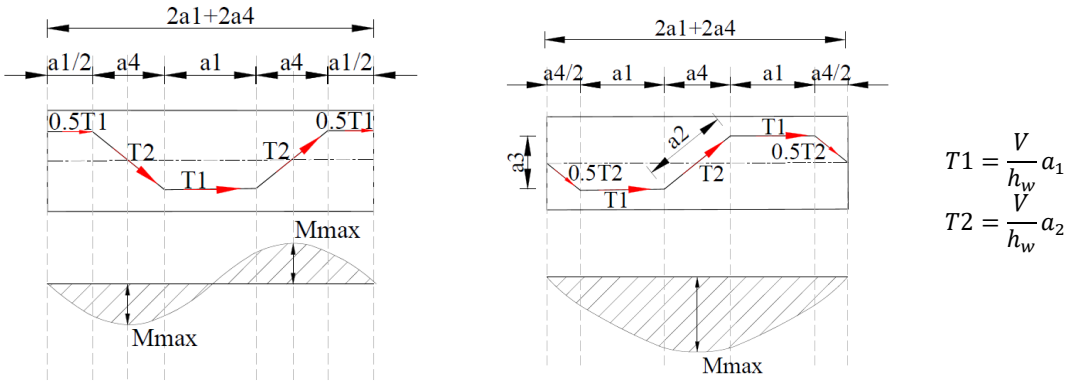

(a) $M_{\max} = \frac{V \cdot a_3}{4 \cdot h_w} \cdot (2 \cdot a_1 + a_4)$ $(b)\ M_{\max} = \frac{V \cdot a_3}{2 \cdot h_w} \cdot (2 \cdot a_1 + a_4)$

Fig. 10 Transverse bending from shear flow according to Kövesdi et al. (10): (a) when the load and supports are located on the flat fold, (b) flow when the load and supports are located on the inclined fold.

Fig. 11 illustrates the separated load effects for Girder 2. This girder has 5.5 corrugation waves per shear span, compared to 4 waves in Girder 1. Due to its longer length, the bending stress is greater, amplifying the effect from the uneven web contribution to the beam section modulus. However, the shear force remains the same as in Girder 1, maintaining a consistent pattern with an amplitude around 10 MPa and the same shape of two half-sine waves per corrugation. Moreover, in both Girders, this bending effect is localized within each corrugation in the shear span.

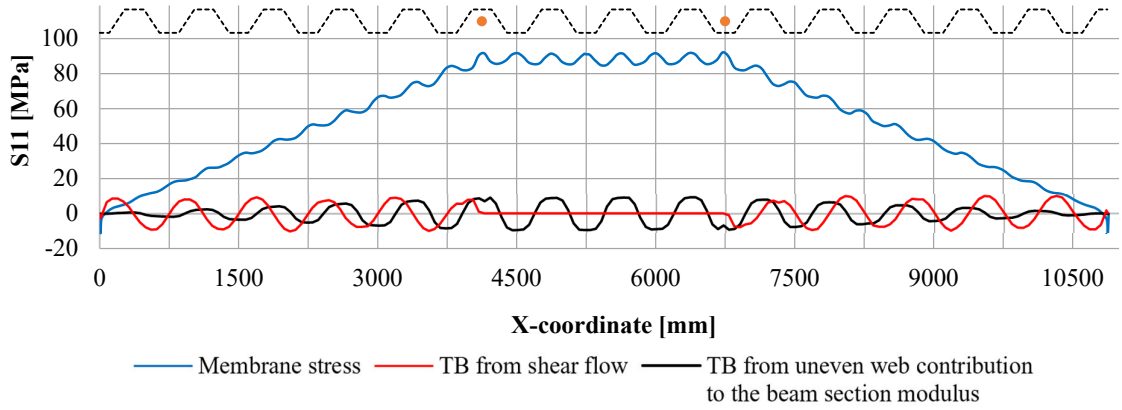

Fig. 11 Separated load effects for Girder 2

Fig. 12 presents the separated load effects for Girder 3. In this girder, the shear span encompasses four corrugations with the load and support applied on the inclined folds. The bending from the uneven web contribution to the beam section modulus follows the same shape as in previous girders, with an amplitude close to that of Girder 1, given its similar bending moment. With reference to shear stress, the load and supports applied to the inclined fold yield in a distinct impact. Specifically, the transverse bending from shear flow displays half-sine wave for each corrugation, see *Fig. 10b*. The magnitude of this transverse bending stress measures roughly twice that in Girders 1 and 2, around 20 MPa. Kövesdi (10) indicates an expected value of approximately 23 MPa for this corrugation arrangement (*Fig. 10b*), which is close to the results obtained using Abbas et al. "Fictitious load

method" (4). The FE analysis predicts a lower value due to the inclusion of the radius in the model, causing a reduction in T1 in *Fig. 10*, as mentioned earlier.

A notable distinction in Girder 3, compared to the previous two girders (Girder 1 and 2), lies in the bending stresses within the constant moment region. These stresses fluctuate around an average value of approximately 3.5 MPa, refer to *Fig. 13*, contrary to theoretical expectations where this value should be zero. This "mean stress" indicates an additional global transverse bending effect induced along the girder which is discussed further in the following sections.

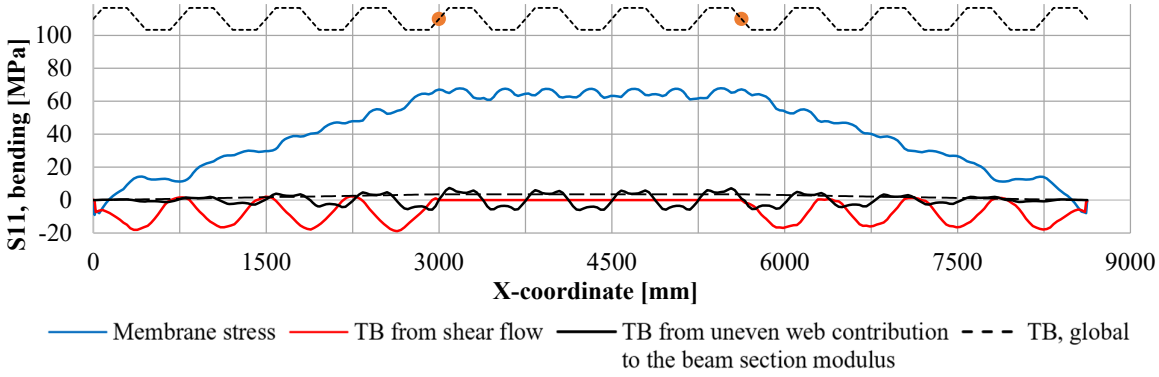

Fig. 12 Separated load effects for Girder 3

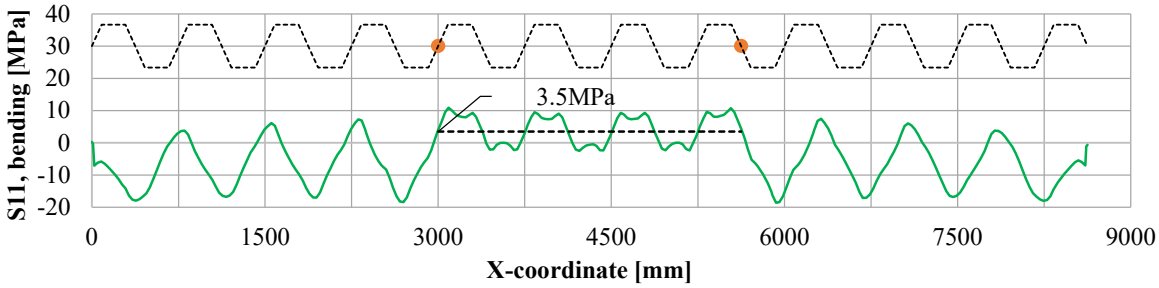

Fig. 13 Total bending stress along Girder 3 (including bending from shear flow and bending from uneven web contribution to the beam section modulus)

Fig. 14 depicts the separated load effects for the last girder (Girder 4). This girder differs from Girder 3 in that the shear span has 4.5 corrugation waves in Girder 4. It is noticeable that the local amplitude of the transverse bending due to shear flow corresponds well with Girder 3, but with an opposite sign due to the flipped corrugations (see first corrugation in *Fig. 14* and *Fig. 12*). However, in Girder 4, beside the load effects observed in Girder 3, a traverse bending from shear flow arises in the pure bending zone which exhibits zero primary shear, refer to *Fig. 14*. This impact had been earlier noted by Abbas et al. (4). Moreover, the global bending effect in this girder is notably larger than previous girder.

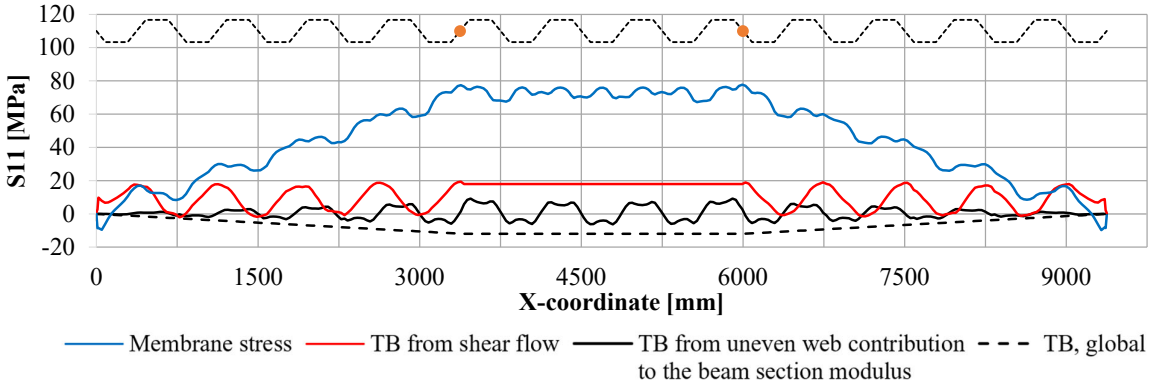

Fig. 14 Separated load effects for Girder 4

2 DISCUSSION ON GLOBAL BENDING EFFECT

After analysing the four girders, the load effects in flanges of girders with corrugated webs can be identified into the following actions (for coordinates, refer to *Fig. 3*):

- Membrane stress: due to bending around beam Y-axis.
- Bending stress around the Z-axis caused by shear flow.
- Local bending stress (moment around the Z-axis) arising from uneven web contribution to the beam section modulus within one corrugation.
- Global bending stress along the girder.

Another observation is that Girder 4 has a greater and opposite global bending stress, with values of -12MPa vs 3.5MPa in Girder 3 *(Fig. 14* and *Fig. 12*). This global effect is dependent on the start and termination of the corrugation in relation to the support and loading points. The sign of this global bending effect is observed to be opposite to the bending from shear flow as can be seen in Girder 4 (*Fig. 14).* The sign of the bending from shear flow depends on the eccentricity direction of the corrugation. For instance, it is opposite in Girder 4 compared to Girder 3 due to the flipped corrugation direction, refer to Girder 3 and 4 in the combined shear-bending region in *Table 3*. This indicates that if the shear spans are asymmetric, the predicted shape for bending from shear and global bending would be as presented in *Fig. 15*.

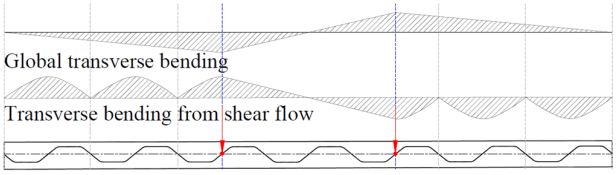

Fig. 15 Illustration of local bending from shear and global bending effects for asymmetric shear spans with non-integer number of corrugation per shear span

3 DISCUSSION ON LOAD EFFECTS FROM FATIGUE DESIGN POINT OF VIEW

The load effects within a single corrugation in the shear span and another in the constant moment region are presented in *Table 3*. Each corrugation wave contains four S-points where fatigue cracks might occur, see *Fig. 16*. The main insights derived from comparing the data in *Table 3* are stipulated below.

In the constant moment region:

- Transverse bending from shear flow affects the constant moment region only when the corrugation number in the shear span is non-integer and the load and supports are applied on the inclined folds. The value of this transverse bending is equal to the local transverse bending from shear in the shear span. This transverse bending increases the stresses in two corrugation corners (S-points) in the constant moment region (A and B for Girder 4, *Fig. 16* and *Table 3*) and decreases the stresses in two corners (C,D) for the same girder.
- When present, this bending and the global transverse bending act in opposite directions, with the transverse bending from shear flow being larger in the studied girders.
- The local transverse bending from the uneven web contribution to the beam section modulus consistently results in compression in the corrugation corners, reducing tension in all four S-points.

In the combined shear-bending region:

- Transverse bending from shear flow exhibits two half- sine waves for Girder 1 (load and supports on the flat fold) and one half-sine wave with double amplitude for Girder 3 and 4 (load and supports on the inclined fold), elevating tensile stress in specific S-points (A' & C' in Girder 1, A & B in Girder 4, *Fig. 16* and *Table 3*).
- The global bending effect exists only when the load and supports are applied on the inclined fold, counteracting the transverse bending from shear flow.

Considering these observations, the corrugations in Girder 4 constant moment region appear to be most critical with respect to load effects at the S-points, displaying the highest bending effects. The global bending effect in this region opposes the transverse bending from shear flow, and therefore in a design situation one needs to consider a combination of membrane stresses and the bending stresses from shear. The latter can be calculated according to Kövesdi or by analyzing the flange as a beam subjected to shear flow resultants.

Table 3 Load effects at the 4 S-points. The results are obtained for the south edge, marked blue in Fig. 16

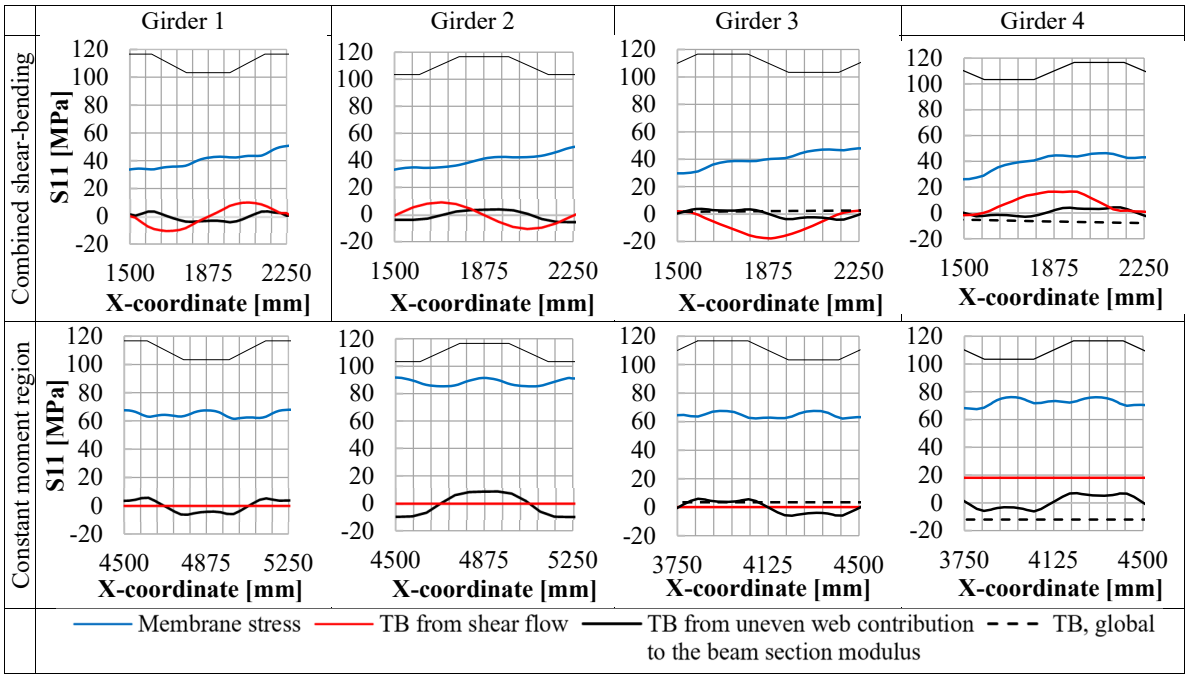

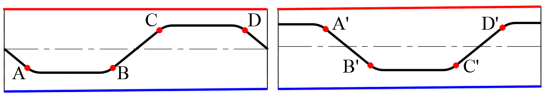

Fig. 16 S-points in corrugated web girder

4 SUMMARY AND CONCLUSIONS

In this study, 4 finite element models loaded in 4-point bending were constructed and validated with hand calculation. The load and the supports were placed on the flat fold in Girder 1 and 2 and on the inclined parts in Girders 2 and 4. Girders 1 and 3 had integer number of corrugation per shear span while Girders 2 and 4 had non-integer number of corrugation per shear span. The load effects under bending and shear are separated and analysed, and the following conclusions are made:

- The stresses in the flange can be divided into four different effects: membrane stress, transverse bending due to shear flow, local transverse bending due to uneven web contribution to the beam section modulus and global transverse bending along the girder.
- The membrane and transverse bending due to uneven web contribution to the beam section modulus effects are always connected and coexist.
- In a 4-point bending loaded girder, where the load and supports are positioned on the inclined folds with a non-integer number of corrugations in the shear span, the constant moment region is influenced by transverse bending due to shear flow. The magnitude of this bending is equal to the maximum effect induced by shear flow in the shear span.
- The positioning of the load and supports on the beam leads to transverse bending due to shear with either two half-sine waves or a single half-sine wave with double the magnitude per

corrugation. Meanwhile, the bending from uneven web contribution to the beam section modulus always compress the flange side closest to the flat fold.

- with respect to fatigue load effect at the S-points, the most critical case is found in the constant moment region when the load and supports are located on the inclined fold and a non-integer number of corrugations is present in the shear span. Herein, the bending from shear exhibits one half-sine wave per corrugation and causes transverse bending in the constant moment region. The membrane stress, transverse bending from shear flow, and transverse bending from uneven web contribution to the beam section modulus combine to give the fatigue design stress in this case.

5 REFERENCES

1. *Stainless steel corrugated web gorders for composite road bridges: Optimization and parametric studies.* **Hlal, Fatima, Amani, Mozhdeh and Al-Emrani, Mohammad.** s.l. : Engineering Structures, 2023, Vol. 302. https://doi.org/10.1016/j.engstruct.2023.117366.

2. **Hlal, Fatima.** *Stainless Steel Corrugated Web Girders for Composite Road Bridges: Concept Evaluation and Flange Buckling Resistance.* s.l. : Chalmers University of Technology, 2023. https://research.chalmers.se/publication/536891.

3. *Bending and shear interaction behavior of girders with trapezoidally corrugated webs.* **Kövesdi, B., Jager, B. and Dunai, L.** s.l. : Journal of Constructional Steel Research, 2016. https://doi.org/10.1016/j.jcsr.2016.03.002.

4. *Analysis of Flange Transverse Bending of Corrugated Web I-Girders under In-Plane Loads.* **H. Abbas, Hassan, Sause, Richard and G. Driver, Robert.** 3, s.l. : Journal of Structural EngineeringArchive, 2007, Vol. 133. https://doi.org/10.1061/(ASCE)0733-9445(2007)133:3(347).

5. *Accordion effect in bridge girders with corrugated webs.* **Inaam, Qazi and Upadhyay, Akhil .** s.l. : Journal of Constructional Steel Research, 2022, Vol. 188. https://doi.org/10.1016/j.jcsr.2021.107040.

6. *Experimental study on fatigue behavior of trapezoidal corrugated-web girders based on T-section members.* **Lewei, Tong, et al.** s.l. : Engineering Structures, 2024, Vol. 298. https://doi.org/10.1016/j.engstruct.2023.117078.

7. *Fatigue of Corrugated-Web Plate Girders: Experimental Study.* **A. Ibrahim, Sherif , W. El-Dakhakhni, Wael and Elgaaly, Mohamed .** 9, s.l. : Journal of Structural Engineering, 2006, Vol. 132. http://dx.doi.org/10.1061/(ASCE)0733-9445(2006)132:9(1371).

8. *Fatigue life of girders with trapezoidally corrugated webs: An experimental study.* **Kövesdi, B. and Dunai, L. .** s.l. : International Journal of Fatigue, 2014, Vol. 64. http://dx.doi.org/10.1016/j.ijfatigue.2014.02.017.

9. *Simplified analysis of flange transverse bending of corrugated web I-girders under in-plane moment and shear.* **H. Abbas, Hassan , Sause, Richard and G. Driver, Robert .** 11, s.l. : Engineering Structures, 2007, Vol. 29. https://doi.org/10.1016/j.engstruct.2007.01.006.

10. *Stress distribution in the flanges of girders with corrugated webs.* **B. , Kövesdi, Jáger, B. and L. , Dunai.** s.l. : Journal of Constructional Steel Research, 2012, Vol. 79. https://doi.org/10.1016/j.jcsr.2012.07.023.

11. *Fatigue of web-flange weld of corrugated web girders: 1. Influence of web corrugation geometry and flange geometry on web-flange weld toe stresses.* **Anami, Kengo , Sause, Richard and Abbas , Hassan H. .** s.l. : International Journal of Fatigue, 2005, Vol. 27. https://doi.org/10.1016/j.ijfatigue.2004.08.006.

12. *Fatigue of web-flange weld of corrugated web girders: 2. Analytical evaluation of fatigue strength of corrugated web-flange weld.* **Anami, Kengo and Sause , Richard.** 4, s.l. : International Journal of Fatigue, 2005, Vol. 27. https://doi.org/10.1016/j.ijfatigue.2004.08.007.

13. **Abaqus Analysis User's Manual 6.11.** http://130.149.89.49:2080/v6.11/books/usi/default.htm.